Research Article

Experimental studies on the effect of obstacle upstream of a Savonius wind turbine

Nabila Prastiya Putri[1] · Triyogi Yuwono[1] · Jasmi Rustam[1] · Prayogi Purwanto[1] · Galih Bangga[2,3]

Abstract
The present studies investigate the performance of a small Savonius vertical axis wind turbine equipped with an upstream obstacle to guide the wind direction. The wind tunnel measurement was carried out in a test facility at the Mechanical Engineering Department, Institut Teknologi Sepuluh Nopember (ITS). The dynamic torque was measured using the brake dynamometer. Several variations of the obstacle orientations were investigated. Two different wind speeds of 2.48 m/s and 7.45 m/s were considered, that correspond to the Reynolds numbers of 30,000 and 90,000, respectively, according to the rotor diameter. It is found from the studies that the mechanical torque and power generated by the rotor are strongly affected by the obstacle. On the other hand, the Reynolds number has no significant impact on the rotor performance.

Keywords Aerodynamics · Experiment · Obstacle · Wind tunnel · Wind turbine

1 Introduction

In the recent years, the demand of renewable energy is steadily increasing due to a shortage of the fossil energy and intensification of the global climate change [1, 2]. Among others, wind has received a great consideration due to its high potential and become the fastest growing industry for renewable energy with more than 30% annual growth rate [1]. Vertical axis wind turbines (VAWTs) received less attention in wind turbine communities because their performance is way smaller than their competitor, horizontal axis wind turbines (HAWTs). However, it is well known that VAWTs are better suited under complex environment involving high uncertainty in wind direction as they require now yaw mechanism, especially because the turbine performance is not affected by the wind direction. There are two main types of VAWT, the Savonius and Darrieus turbines. The latter is actually more preferred because this turbine is working as a lift type machine that is more efficient. However, its self-starting behaviour is poor. On the other hand, the first-mentioned type has a good self-starting behaviour but weaker performance.

Several studies have been carried out to investigate the performance of vertical axis wind turbines. Dabiri [3], Jang et al. [4], Kinzel et al. [5], Li and Calisal [6] and Bangga et al. [2] pointed out that the performance of a VAWT in a complete isolation can be different with the turbine operating in closely spaced wind park. They concluded that the power of the turbine increases up to 25% if two turbines are arranged close to each other in side-by-side configuration. The power improvement is caused by the increased velocity between the two rotors. This shows that controlling the incoming wind flow is essential for improving the turbine performance.

Savonius turbines have been investigated in the past by numerous authors. A very comprehensive review, for example, was written by Akwa et al. [7]. This work highlights the performance of Savonius rotors (efficiency

✉ Nabila Prastiya Putri, nabilaprastiyaputri@gmail.com; Triyogi Yuwono, triyogi@me.its.ac.id; Jasmi Rustam, jasmirustam4@gmail.com; Prayogi Purwanto, prayogiadist@gmail.com; Galih Bangga, bangga@iag.uni-stuttgart.de | [1]Mechanical Engineering Department, Institut Teknologi Sepuluh Nopember (ITS), Surabaya, Indonesia. [2]Institute of Aerodynamics and Gas Dynamics (IAG), University of Stuttgart, Stuttgart, Germany. [3]Center for Renewable and Sustainable Energy Research (CRSER), Surabaya, Indonesia.

SN Applied Sciences (2019) 1:1216 | https://doi.org/10.1007/s42452-019-1253-2

Received: 16 November 2018 / Accepted: 10 September 2019 / Published online: 13 September 2019

ranging from 0.05 to 0.3) and their unique abilities like simple construction, high startup ability and low noise. Nakajima et al. [8], explained the physics of a Savonius rotor by the main flows that occur on the rotor buckets during the operation. From these studies, the main flow patterns affecting the performance of the rotor are characterized. These complex flow characteristics make the theoretical prediction of the Savonius performance very difficult [9]. As alternatives, numerical predictions were performed as attempts to solve this issue [10]. As there is no reliable analytical method for predicting the performance of Savonius turbines, experimental or numerical research works must be conducted [7].

The low performance of the Savonius rotor can be improved by adding an obstacle that shields the returning blade. Many authors have adopted various techniques to maximize the performance and to improve the starting torque behaviour of the Savonius turbines, for example by guide vanes [11], V-Plate deflector [12] and deflector plate [13, 14]. Mohamed et al. [15] evaluated the effects of blade number on the performance of a Savonius turbine using CFD. They equipped the rotor with a flat plate upstream of the returning blade. They concluded that the upstream obstacle is able to improve the generated power up to 27.3% and 27.5% for the two-bladed rotor and three-bladed rotor, respectively. They further extended the studies with the variation of the plate geometry in [16]. It was found that the power of the studied Savonius turbine enhances up to 38.9% at a tip speed ratio (TSR) of 0.7 and up to 75.4% at a TSR of 1.4. Priandika [17] recently investigated the effects of an upstream obstacle on the generated power of a Savonius turbine using an experimental approach. The studies varied the obstacle angle, its configuration and the inflow wind speed. It was found that the opening angle of 40° generates the highest power production (1.67 times) among the other variations for the Reynolds number (Re) of 60,000. However, if the Reynolds number is 90,000, the maximum power is generated at an opening angle of 0°. This inconsistency seems to be related to the blockage effects that were not considered in the measurement. Triyogi et al. [18] numerically investigated the effect of a single obstacle upstream of the returning blade on the pressure field surrounding a Savonius turbine, where the turbine was set in the standstill situation. They concluded that the generated power of the turbine may depend on the obstacle width and the operating *Re* as the pressure field changes considerably. However, when the obstacle width is too large, e.g., for $L/D = 2.0$ at $Re = 90{,}000$, a large portion of the area in the upstream vicinity of the returning blade is characterized by the small pressure level. This causes the flow to pass through the area rather than pushing the advancing blade and might reduce the rotor performances. These conclusions were confirmed in a later experimental study [19]. They found that the turbine performance actually is smaller than the baseline case without an obstacle for $L/D > 1.4$ at $Re = 90{,}000$. The turbine power was only 60.8% of the turbine without the installed obstacle for $L/D = 1.83$ at $Re = 90{,}000$.

Golecha et al. [20] further studied the influence of an obstacle shielding the returning blade. Eight different positions were investigated. It was shown that the performance of the turbine could be increased by 50% when the configuration is optimal. The deflector plate acts as an obstacle for the incoming flow towards the returning blade that increases the net torque generated by the rotor. Eight different positions of the obstacle were evaluated in these studies. This group further evaluated the influence of an additional flow deflector nearby the advancing blade in [21]. The power coefficient increased to 0.35, that is significantly higher than the open rotor of 0.14. The dual rotor system performance, as also investigated in [2–6], were attempted to be improved by using a flat plate deflector by Kim and Gharib [22]. It was concluded that the power output enhancement with the installed deflector is dependent on the width and height of the deflector and the relative turbine position. Tartuferi et al. [23] emphasized that redesigning the blade sections and the curtain system could enhance the power generated from the turbine. The blade geometry was redesigned based on the common principle of imposing a considerable increase of the mean camber line in order to design a section of suitable curvature for replacing the traditional semi-cylindrical blade geometry. They further equipped the rotor with the non-conventional conveyor-deflector curtain system. Both modifications were improving the rotor performance.

It can be seen that there is still an open room for improvement and further studies. The present studies are conducted especially as the effect of opening angle of the upstream deflector was not yet widely evaluated in detail. The present work is intended to further elaborate the investigations experimentally. The main objectives of the studies are to evaluate the effects of upstream obstacle on the aerodynamic performance of the turbine and to determine the optimum angle required to guide the flow towards the turbine.

2 Research methodology

The turbine was mounted in front of an axial fan that can rotate up to 2850 rpm. The fan speed is adjustable to obtain the desired wind speed. To minimize the effects of inflow turbulence, a square-honeycomb was installed between the two apparatuses. The honeycomb size is

508 mm with the mesh size of 16 per square inch. This approach was adopted to avoid swirl flow as recommended by Bradshaw [24]. Detailed overview of the turbine and the measurement equipments is given in Figs. 1 and 2. The wind flows through the honeycomb and reaches the turbine at a distance of 3500 mm. The turbine is a Savonius type with a blade radius of 101.6 mm. The height of the turbine is 300 mm and the overlap diameter of the shaft is 13 mm. Thus, the effective diameter of the turbine is 190.2 mm. The obstacle is located at 120 mm upstream of the turbine and its opening angle can be adjusted in the experiment. The length of the obstacle is 143.6 m, thickness of 3 mm and height is 300 mm that is the same as the turbine height.

The rotation of the turbine was recorded using a non-contact optical tachometer OMEGA HHT12 with the measurement range of 5 to 99,999 rpm. The accuracy of the rotational speed measurement is 0.001 to 0.1 rpm. The wind speed was measured using an anemometer OMGA HHF92A with the measurement range of 1.5–35 m/s and accuracy of 0.01 m/s. Note that two measurement strategies for the mechanical torque were carried out. First, the static torque was measured using a torque meter LUTRON TQ-8800 with the measurement range of 0.1–1.0 N cm. Second, the dynamic torque was recorded using a brake dynamometer. The latter is preferred as it is more accurate and was recommended Mahmoud et al. [25]. Thus, the main results of the present studies were obtained from the dynamic torque approach.

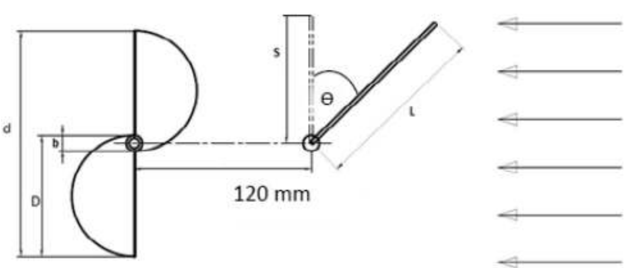

Fig. 1 Schematic illustration of the turbine and flat plate obstacle upstream of the returning blade

3 Results and discussion

In this section, the obtained experimental results are presented and the occurring physical phenomena are discussed. Figure 3 shows the airflow distribution in front of the rotor that was measured using anemometer. The distributions of the vertical and horizontal profiles are presented. The measurement took place at 700 mm upstream of the rotor at five different positions along the horizontal and vertical axes. It can be noticed that the honeycomb makes the inflow more uniform than the case without the installed honeycomb. The installed honeycomb also reduces the turbulence levels at the inlet. However, this was not measured and is not a topic of interest for the present work.

Figure 4 presents the effects of obstacle angle on the rotational speed of the turbine represented as a dimensionless quantity of the tip speed ratio, that can be formulated as:

$$TSR = \frac{\omega R}{U_\infty}, \quad (1)$$

where ω represents the rotational frequency, R represents the effective blade radius and U_∞ is for the undisturbed wind velocity. It can be seen clearly that the obstacle opening angle has a minimum effect on TSR. This shows that the rotor rotation is not affected strongly by the equipment. It can be seen that the Reynolds number also has a small influence on TSR. Note that the dynamic measurement was carried out when the rotor is under loaded situation, i.e. when the weight is applied on the dynamometer.

Figure 5 shows the measured dynamic driving moment coefficient of the rotor. This coefficient is defined as:

$$C_M = \frac{M}{\frac{1}{2}\rho_\infty U_\infty^2 SR}, \quad (2)$$

where M is the measured dynamic torque, ρ_∞ is the freestream density and S is the cross-sectional area. It becomes evident that the generated torque depends on the obstacle opening angle and the Reynolds number. From Fig. 5 (upper), it is shown that the maximum effect

Fig. 2 Schematic view of the measurement apparatuses

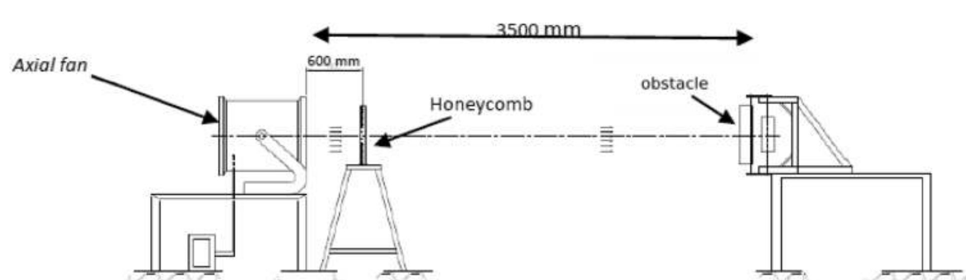

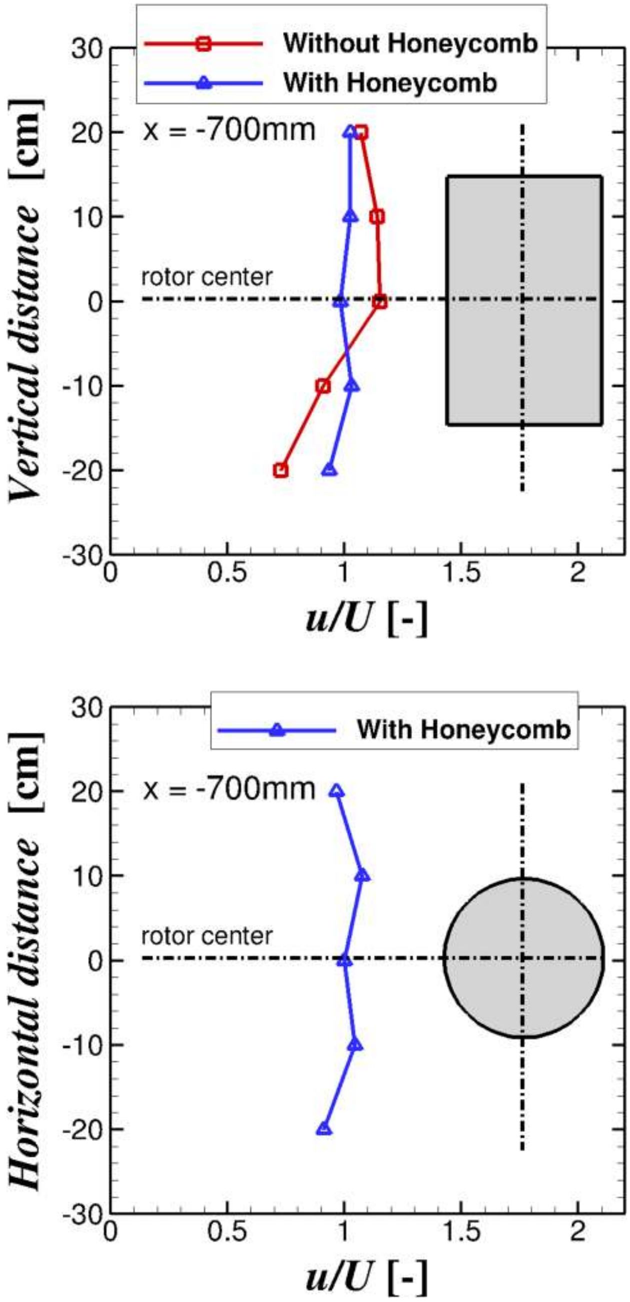

Fig. 3 Flow distribution in front of the turbine

on C_M occurs for $Re = 30{,}000$ at 40°, and in comparison to $Re = 90{,}000$ the moment coefficient is generally higher. It is shown that both Reynolds numbers present the same trend. When observing the relative increase of the moment coefficient to the baseline case without the obstacle, Fig. 5 (lower) also shows that a similar trend holds for both Reynolds numbers. It can be clearly seen that the torque has its maximum value at $\theta = 40°$ regardless of the Reynolds number, indicating an optimum opening angle of the obstacle.

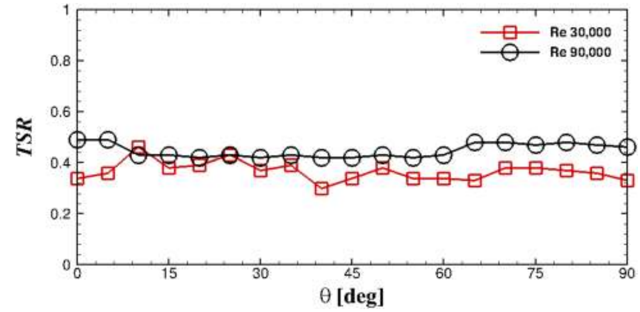

Fig. 4 Tip speed ratio distributions as a function of the obstacle opening angle at maximum power coefficient

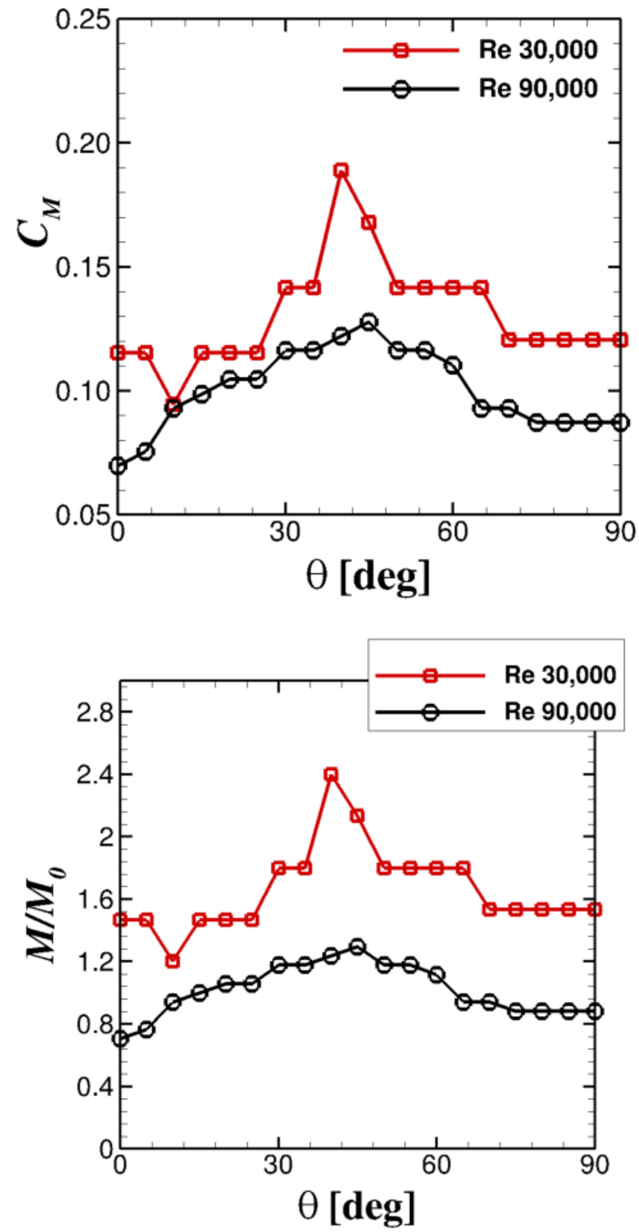

Fig. 5 Torque coefficient (upper) and increased torque relative to the baseline case (lower)

In Fig. 6, the power coefficient of the turbine is presented. This variable is defined as the relative energy extracted from the wind and can be formulated as

$$COP = \frac{M\omega}{\frac{1}{2}\rho_\infty U_\infty^3 S} \times 100\%. \tag{3}$$

It can be seen now that the power generated from the rotor, Fig. 6 (upper), for $Re = 30{,}000$ is similar with $Re = 90{,}000$. The generated power for $Re = 30{,}000$ is of the similar order as $Re = 90{,}000$. In a similar line, there is only a slight deviation on the increased power relative to the baseline case as depicted in Fig. 6 (lower), indicating that the Reynolds number has actually only a minor influence on the improved performance. Similar to the observation for the torque, the power of the rotor depends strongly upon the obstacle opening angle. However, the maximum power is not generated exactly as when the torque is maximum at $\theta = 40°$, but this occurs at a slightly higher angle at $\theta = 45°$. This shows that the generated power of the turbine is not always in line with the dynamic torque acting on the shaft. Interestingly, in contrast to the moment coefficient in Fig. 5, the power coefficient is not affected by the Reynolds number. This difference is attributed to the variation in the rotational speed achieved at the maximum CoP at the respective configuration.

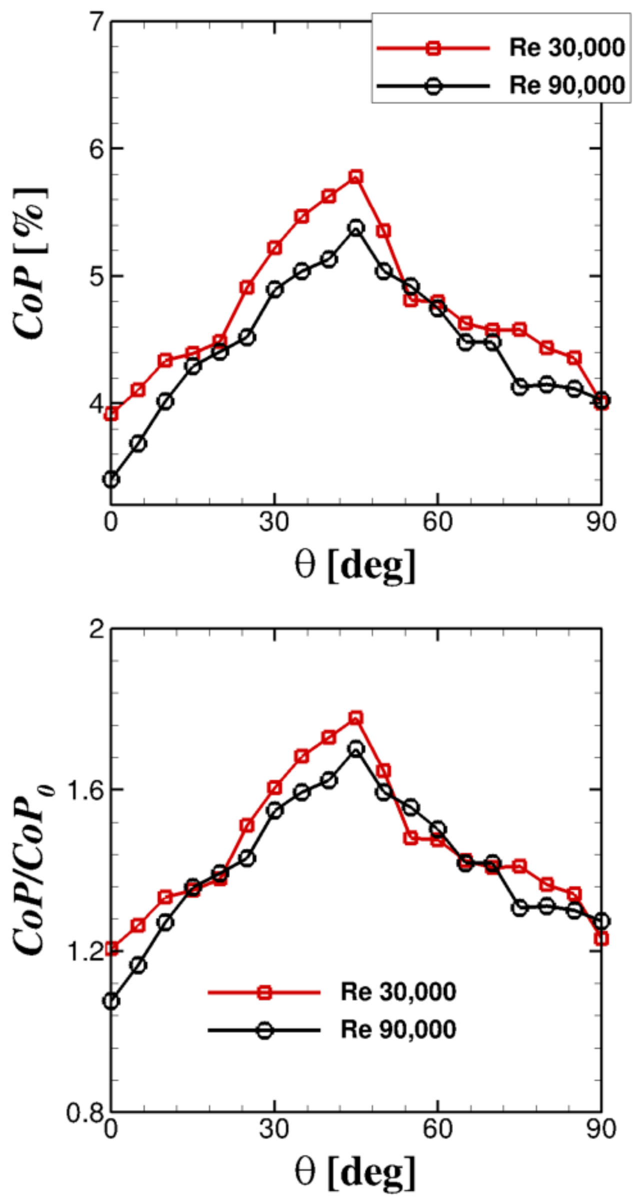

Fig. 6 Power coefficient (upper) and increased power relative to the baseline case (lower)

Generally, the power coefficient generated by a Savonius rotor is larger than 0.1, especially when the rotor is equipped with an upstream obstacle. In the present work, the magnitude is smaller. One may think that the size of the turbine could play a significant role. The high solidity of the turbine could deteriorate the performance due to the blockage effects of the flow through the rotor plane affecting the inductions, for example see [26]. On the other hand, friction can be large for this case, which may further contribute to the reduced performance.

Figure 7 shows the static torque testing for the Savonius turbine when the rotor is at idle position without loading. The measurements were calculated by the static digital torque meter which was installed at the rotor shaft and when the rotor blade position was perpendicular to the direction of air flow.

It can be depicted from Fig. 7 (upper) that the trend of the static torque for two different Reynolds numbers is very similar. It shall be noted, however, that the magnitudes are completely different. The measured static torque levels increase when the opening angle of the obstacle enlarges up to 30°. A further increase of the opening angle causes a stronger blockage effect that reduces the static torque level for all investigated cases. Despite that, a more gradual reduction of the static torque level is observed for the operating Reynolds number of 90,000. This is actually beneficial for the turbine itself because the operating range is wider, avoiding severe impacts when faulty of opening angle selection occurs in practice. The main reason for the higher level of static torque at a higher Reynolds number is that the air velocity is increasing considerably. Note that the Reynolds number is directly proportional to the wind speed. In Fig. 7 (lower), one could observe that the Reynolds number has only little influence on the static torque coefficient of the rotor.

While the velocity increases, at the same time the difference in drag force between the advancing and returning blades also increases. Note that the torque is mainly generated by the drag force for this type of turbine. The

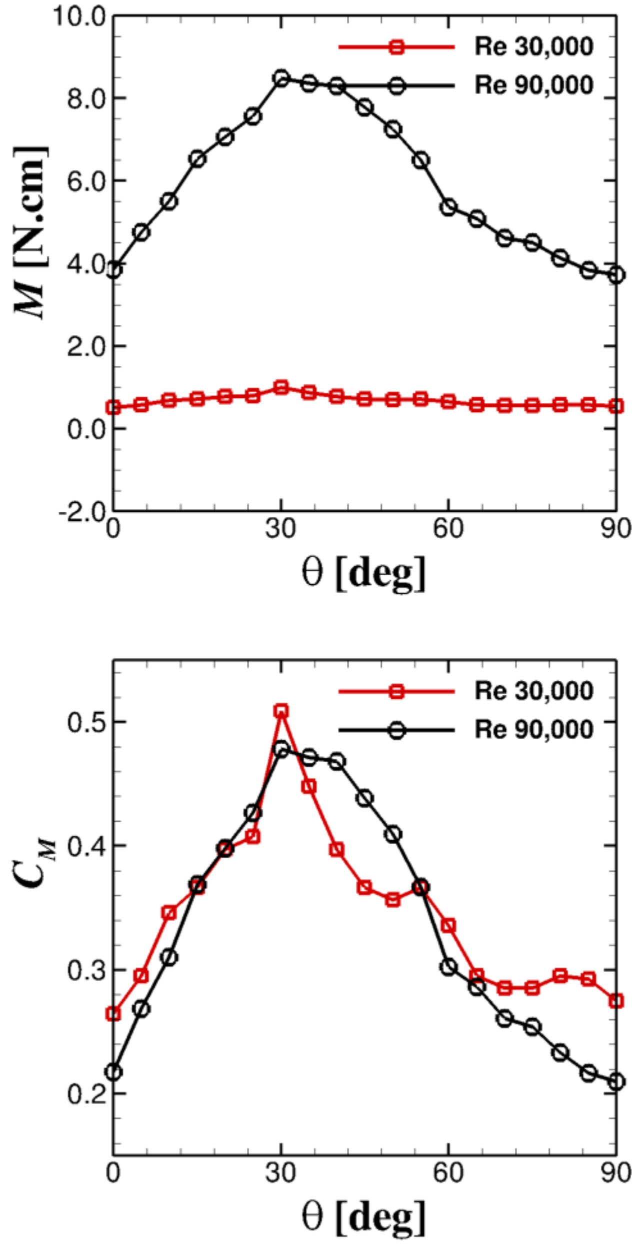

Fig. 7 Static torque measurement as a function of the opening obstacle angle

level of the static torque increases as long as there is an increase in the drag force difference between the two blades and it depends on the configuration of the obstacle plate that change the location of the center of force on the blade. The maximum static torque occurs at an angle value of 30°. The torque arm is longer at this position. After the optimum angle is passed, the reduction of the static torque the center of the drag force is shifted causing a shorter torque arm and it leads to the smaller torque levels.

4 Conclusions and remarks

Experimental studies have been carried out to assess the capability of an obstacle located upstream of a Savonius wind turbine to improve the power generated by the rotor. The investigations highlight several aspects that are useful for wind energy communities. The obstacle and the Reynolds number have a small influence on the rotational speed of the loaded turbine. On the other hand, the torque of the turbine is strongly influenced by the opening angle of the obstacle. The improvement of the torque value relative to the baseline case without an obstacle is less affected by the Reynolds number. The studies reveal that the obstacle opening angle strongly influences the acting torque, where the maximum torque takes place at $\theta = 40°$ regardless of the Reynolds number. However, this position is slightly shifted to $\theta = 45°$ for the generated power. However, relative to the baseline case, the Reynolds number has a minor influence on the increased power and it is affected mainly by the obstacle opening angle. The static torque results reveal that the rotor torque increases with increasing opening obstacle angle up to the angle of 30° for all investigated inflow conditions, then it reduces again when the angle increases further.

Further improvements of the power production might be still possible if the motion of the upstream obstacle can be actively controlled, for instance, for enhancing the starting behavior or for maximizing the maximum torque generation. It was shown in previous studies that providing additional mass flow on the system could delay separation and might be beneficial to further control the power improvement capability of the proposed approach. Future studies might be directed to the 3D simulation of the turbine by a scale resolving technique as it was proven to be able to accurately capture flow separation and predict the loads on the rotor especially regarding the 3D effects. Moreover, confirming the results in the open-field measurement campaign is of importance because many parameters are not directly comparable with the laboratory environment. Therefore, experimental studies in this direction are strongly recommended.

Acknowledgements The authors would like to express their gratitude to the Mechanical Engineering Department, Institute Teknologi Sepuluh Nopember for providing the wind tunnel facility.

Compliance with ethical standards

Conflict of interest The authors declare that there is no conflict of interest regarding the publication of this paper.

References

1. Bangga G, Hutomo G, Wiranegara R, Sasongko H (2017) Numerical study on a single bladed vertical axis wind turbine under dynamic stall. J Mech Sci Technol 31(1):261–267
2. Bangga G, Lutz T, Krämer E (2018) Energy assessment of two vertical axis wind turbines in side-by-side arrangement. J Renew Sustain Energy 10(3):033303
3. Dabiri J (2011) Potential order-of-magnitude enhancement of wind farm power density via counter-rotating vertical-axis wind turbine arrays. J Renew Sustain Energy 3(4):043104
4. Jang C, Kim Y, Kang S, Lee J (2016) An experiment for the effects of the distance and rotational direction of two neighbouring vertical Savonius blades. Int J Energy Res 40(5):632–638
5. Kinzel M, Mulligan Q, Dabiri J (2012) Energy exchange in an array of vertical-axis wind turbines. J Turbul 13(1):N38
6. Li Y, Calisal S (2010) Estimating power output from a tidal current turbine farm with first-order approximation of hydrodynamic interaction between turbines. Int J Green Energy 7(2):153–163
7. Akwa J, Vielmo H, Petry A (2012) A review on the performance of Savonius wind turbines. Renew Sustain Energy Rev 16(5):3054–3064
8. Nakajima M, Iio S, Ikeda T (2008) Performance of double-step Savonius rotor for environmentally friendly hydraulic turbine. J Fluid Sci Technol 3:410–419
9. Fernando M, Modi V (1989) A numerical analysis of the unsteady flow past a Savonius wind turbine. J Wind Eng Ind Aerodyn 32(3):303–327
10. D'Alessandro V, Montelpare S, Ricci R, Secchiaroli A (2010) Unsteady aerodynamics of a Savonius wind rotor: a new computational approach for the simulation of energy performance. Energy 35(8):3349–3363
11. Hayashi T, Li Y, Hara Y (2005) Wind tunnel tests on a different phase three-stage Savonius rotot. JSME Int J Ser B 48:9–16
12. Shaughnessy B, Probert S (1992) Partially-blocked Savonius rotor. Appl Energy 43(43):239–249
13. Huda M, Selim M, Sadrul A, Islam M (1992) The performance of an S-shaped Savonius rotor with a deflecting plate. RERIC Int Energy J 15:25–32
14. Ogawa T, Yoshida H, Yokota Y (1989) Development of rotational sped control systems for a Savonius-type wind turbine. J Fluids Eng 111:53–58
15. Mohamed MH, Janiga G, Pap E, Thevenin D (2010) Optimization of Savonius turbines using an obstacle shielding the returning blade. Renew Energy 35:2618–2626
16. Mohamed MH, Janiga G, Pap E, Thevenin D (2011) Optimal blade shape of a modified Savonius turbine using an obstacle shielding the returning blade. Energy Convers Manag 52:236–242
17. Priandika Y (2016) Experimental study on the effect of disturbance plate angle in front of returning blade of savonius type wind turbine to the turbine performance. Case study for the ratio length of disturbance plate relative to the diameter of turbine (L/D) = 1.414" Sepuluh Nopember Institute of Technology
18. Yuwono T, Latip A, Putri N, Muhammad U, Mazhilna E, Ariyanto C, Andaryani U, Fauzi A (2018) Numerical study on the effect of width of single curtain on the performance of Savonius wind turbine. In: MATEC web of conferences, vol 154, p 01110
19. Yuwono T, Latip A, Putri N, Ubaidillah M, Mazhilna E, Ariyanto C, Andaryani U, Fauzi A, Widodo W, Dwiyantoro B (1983) The effect of width of single curtain on the performance of Savonius wind turbine. In: AIP conference proceedings, vol 2018, p 020023
20. Golecha K, Eldho T, Prabhu S (2011) Influence of the deflector plate on the performance of modified Savonius water turbine. Appl Energy 88:3207–3217
21. Golecha K, Eldho T, Prabhu S (2012) Performance study of modified Savonius water turbine with two deflector plates. Int J Rotat Mach 2012:1–12
22. Kim D, Gharib M (2013) Efficiency improvement of straight-bladed vertical-axis wind turbines with an upstream deflector. J Wind Eng Ind Aerodyn 115:48–52
23. Tartuferi M, D'Alessandro V, Montelpare S, Ricci R (2015) Enhancement of Savonius wind rotor aerodynamic performance: a computational study of new blade shapes and curtain systems. Energy 79:371–384
24. Bradshaw P (1975) The design of low-speed wind tunnel. National Physical Laboratory, Teddington
25. Mahmoud NH, EL-Haroun A, Wahba E, Nasef MH (2010) An experimental study on improvement of Savonius rotor performance. Renew Energy 35:2618–2626
26. Bangga G, Dessoky A, Lutz T, Krämer E (2019) Improved double-multiple-streamtube approach for H-Darrieus vertical axis wind turbine computations. Energy 182:673–688